Supplemental Information

Targeted inhibition of EGFR and glutaminase induce metabolic crisis in EGFR mutant lung adenocarcinoma.

Milica Momcilovic[1§], Sean T. Bailey[1§], Jason T. Lee[3], Michael C. Fishbein[2], Clara Magyar[2], Daniel Braas[3,6], Thomas Graeber[3,5,6], Nicholas J. Jackson[7], Johannes Czernin[3,5], Ethan Emberley[9], Matthew Gross[9], Julie Janes[9], Andy Mackinnon[9], Alison Pan[9], Mirna Rodriguez[9], Melissa Works[9], Winter Zhang[9], Francesco Parlati[9], Susan Demo[9], Edward Garon[4,5], Kostyantyn Krysan[1], Tonya C. Walser[1], Steven M. Dubinett[1,2,5], Saman Sadeghi[3], Heather Christofk[3,5,6,8] and David B. Shackelford[1,5*]

Inventory of Supplemental Information

Supplemental data
Figure S1 related to Figure 1
Figure S2 related to Figure 2
Figure S3 related to Figure 3
Figure S4 related to Figure 4
Supplemental Table

Supplemental Experimental Procedures

Supplemental References

Supplemental Figures

Supplemental Figure 1

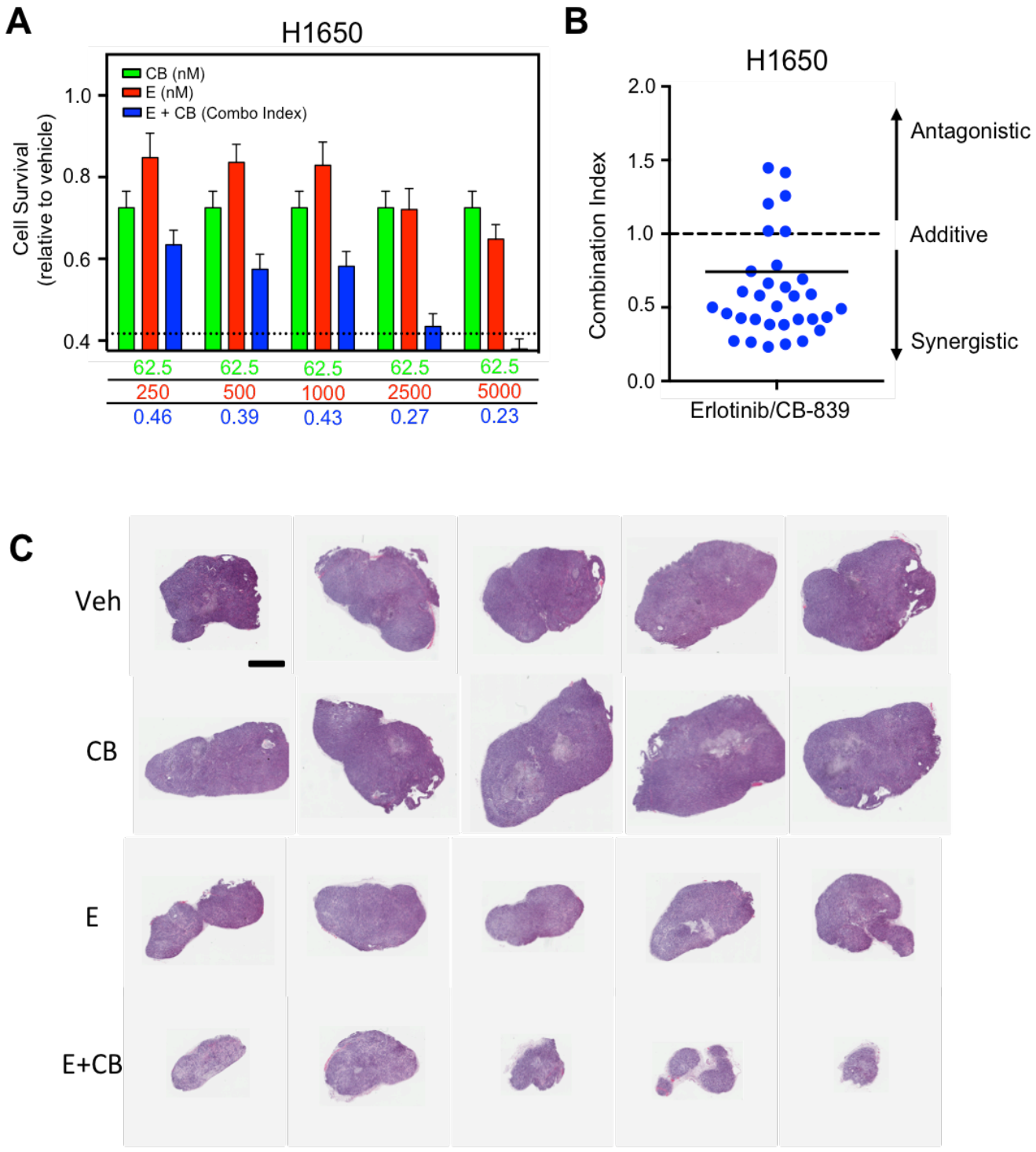

Supplemental Figure 1 related to Figure 1. Combination index of E+CB treated H1650 NSCLC cells and tumor histology of HCC827 xenografts after treatment.

(A) H1650 cell line was incubated with indicated concentrations of CB-839 (CB, green bar), Erlotinib (E, red bar), or Erlotinib + CB-839 (E + CB, blue bar). (B) Combination index for H1650 cell line treated with Erlotinib and CB-839. (C) Immunohistochemistry images from tumors (n=5/group) stained with hematoxylin and eosin. Treatments included vehicle (Veh), CB-839 (CB) 200 mg/kg/bid/p.o., Erlotinib (E) 12.5 mg/kg/qd/p.o., Erlotinib + CB-839 (E+CB). Black scale bar = 2 mm.

Supplemental Figure 2

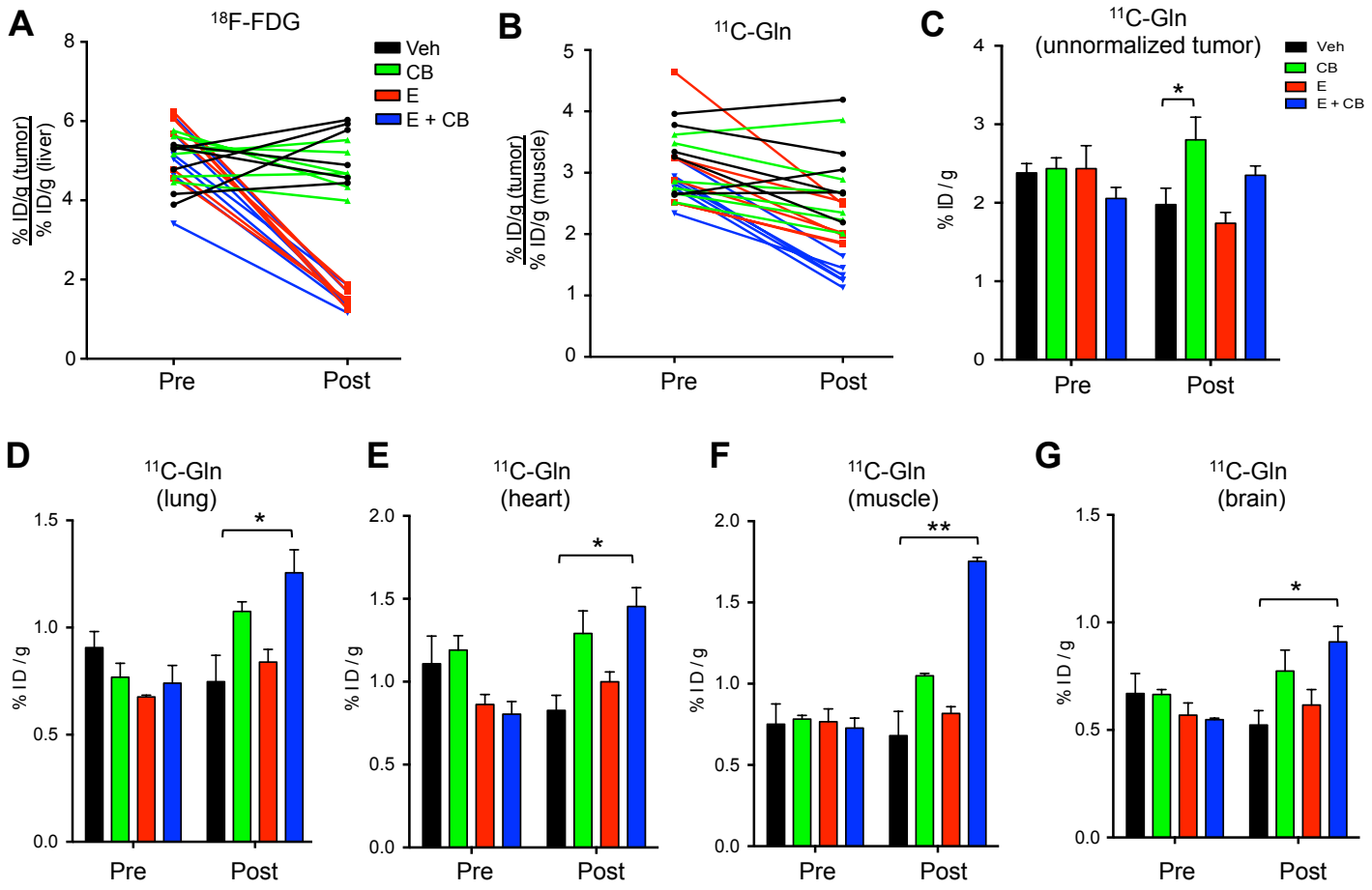

Supplemental Figure 2 related to Figure 2. ^{18}F-FDG and ^{11}C-Glutamine uptake in tumors and mouse tissues.
(A and B) Quantification of ^{18}F-FDG and ^{11}C-Gln uptake by tumors plotted as individual values pre and post treatment (n=6/group) of percent injected dose/gram (%ID/g). (C-G) Uptake of ^{11}C-Gln was quantified for (C) tumors (n=6/group) (D) lung, (E) heart, (F) muscle and (G) brain (n=3/group) by percent injected dose/gram (%ID/g) for vehicle (Veh) (black), CB-839 (CB) 200 mg/kg/bid/p.o. (green), Erlotinib (E) 12.5 mg/kg/qd/p.o. (red), Erlotinib + CB-839 (E+C) (blue).

Supplemental Figure 3

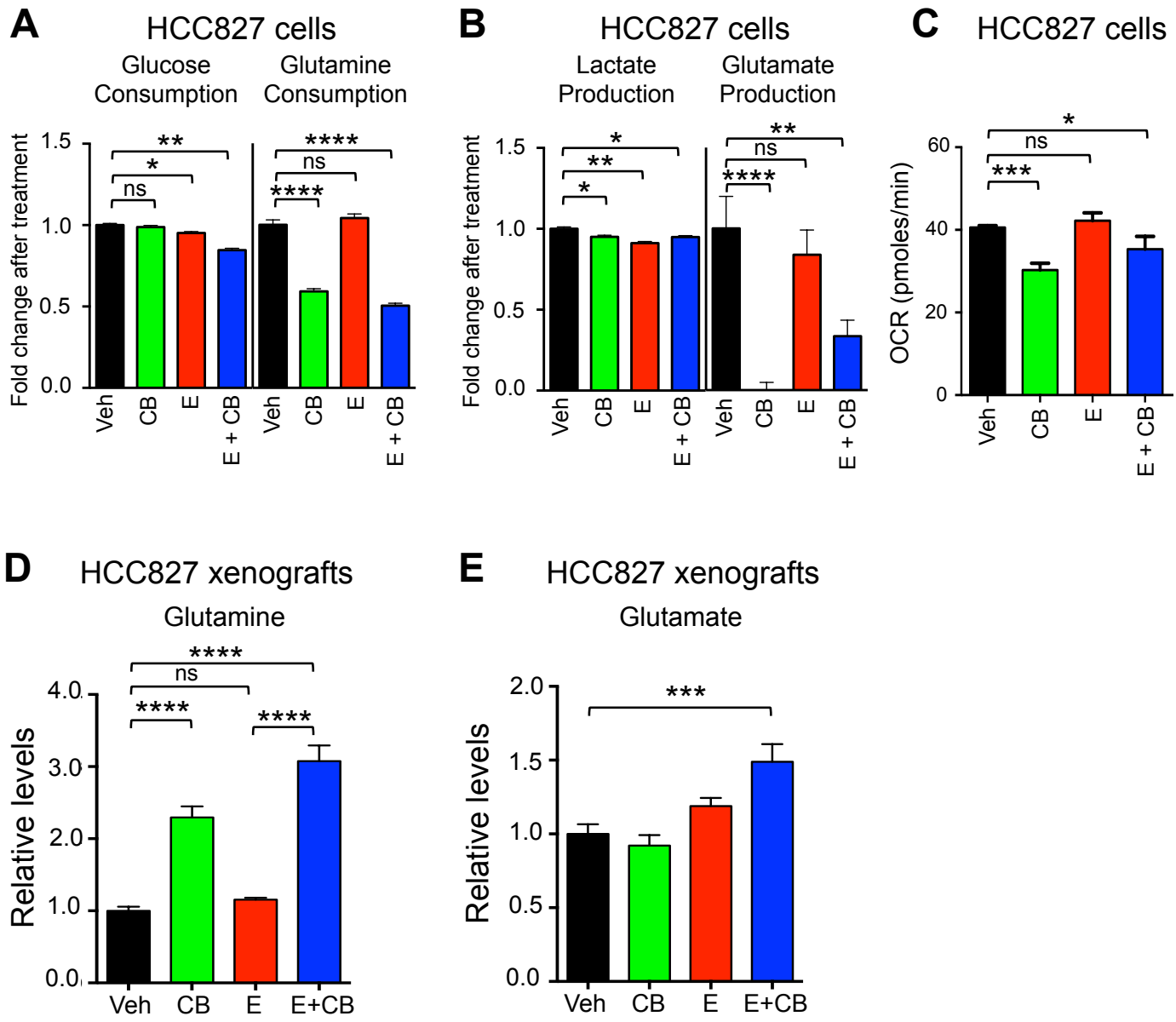

Supplemental Figure 3 related to Figure 3. Metabolite analysis in H1650 NSCLC cells and HCC827 xenograft tumors.

(A and B) Metabolite analysis of H1650 cell line treated with Vehicle (Veh, black bar), CB-839 (CB, green bar), Erlotinib (E, red bar) and Erlotinib + CB-839 (E + CB, blue bar). Fold change in metabolites relative to Vehicle are plotted for (A) Glucose and Glutamine consumption, and for (B) Lactate and Glutamate production. (C) H1650 cell line was incubated with Vehicle (Veh, black bar), CB-839 (CB, green bar), Erlotinib (E, red bar) and Erlotinib + CB-839 (E + CB, blue bar) and oxygen

consumption rate (OCR) was measured. (D-E) Relative metabolite levels of pooled glutamine and pooled glutamate extracted from tumors following treatment and quantified using LC/MS.

Supplemental Figure 4

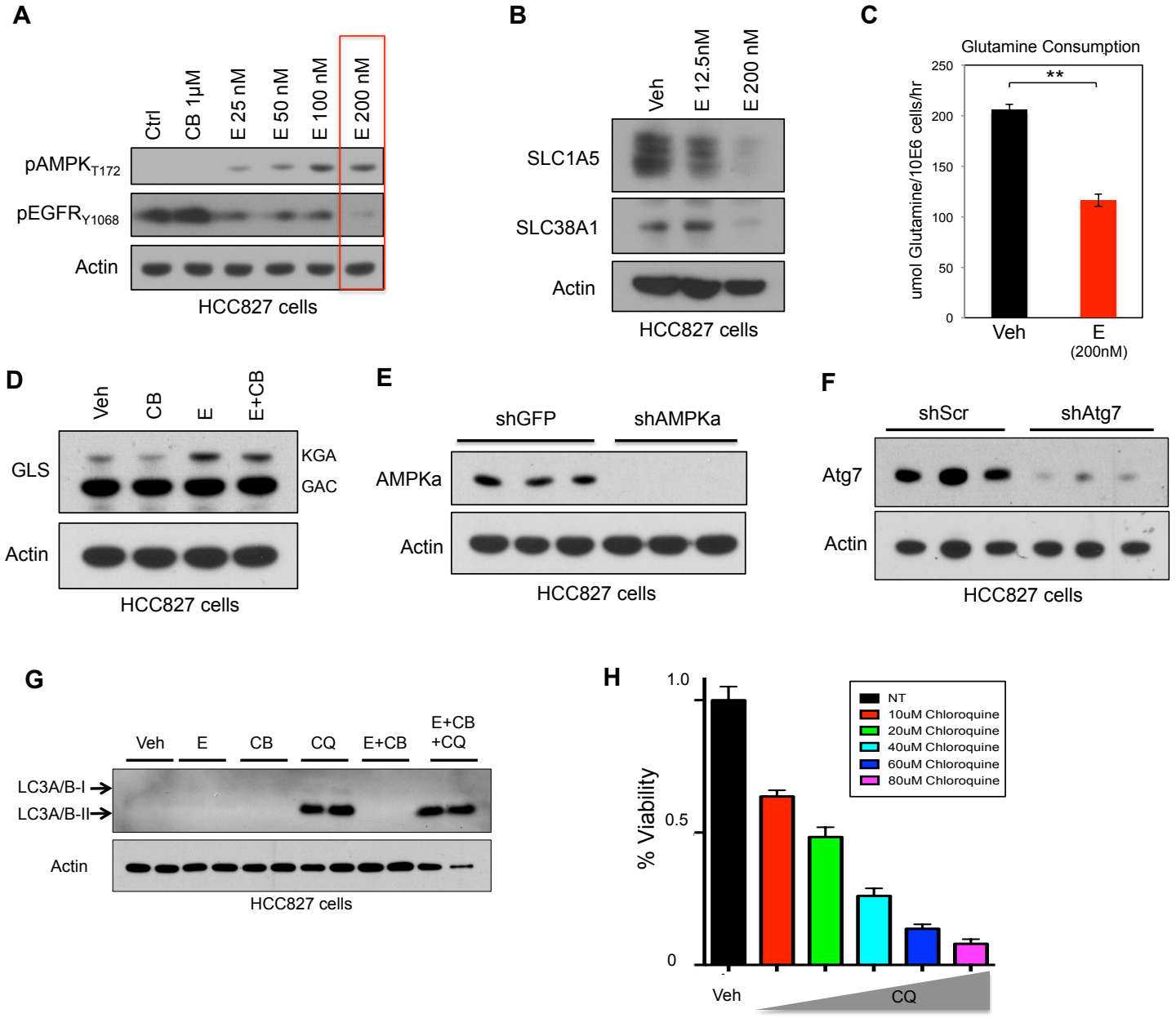

Supplemental Figure 4 related to Figure 4. Autophagy contributes to basal cell growth in HCC827 cell line.

(A-B) Lysates from HCC827 cells were immunoblotted with the indicated antibodies. (C) Glutamine consumption measured in HCC827 cells treated with vehicle (Veh) or 200nM erlotinib (E). (D) Lysates from HCC827 cells were probed with an antibody against glutaminase (GLS) that recognizes both KGA and GAC isoforms. Cells were treated as in Figure 4A and 4B. (E and F) Knockdown of (E) AMPKa1/a2 and (F) Atg7 in HCC827 cells was confirmed by immunoblotting using indicated

antibodies. (G) Lysates from cells treated as in Figure 4H were probed with indicated antibodies. (H) HCC827 cells were treated with Vehicle (Veh) or increasing concentrations of Chloroquine for 72hr.

Table S1, related to Figure 2C, 2D

Table S1. Statistical analysis of normalized values for mice pre and post 18F-FDG and 11C-Gluatmine PET imaging

Mixed-effects linear regression using Restricted Maximum Likelihood Estimation was used. Mouse was fit as a random intercept.

	18F-FDG		11C-Glutamine	
Comparison	**Pre** ***p-value***	**Post** ***p-value***	**Pre** ***p-value***	**Post** ***p-value***
Veh vs E	0.1424	<.0001	0.8098	0.0216
Veh vs CB	0.4933	0.0607	0.4898	0.3773
Veh vs E+CB	0.703	<.0001	0.292	<.0001
E vs CB	0.4342	<.0001	0.6528	0.1573
E vs E+CB	0.2776	0.8526	0.4162	0.0458
CB vs E+CB	0.7613	<.0001	0.7165	0.0006

Supplemental Experimental Procedures

Xenograft experiments

Animal studies were approved by the UCLA Animal Research Committee and were carried out according to the guidelines of the Department of Laboratory Medicine at UCLA. White SCID mice (7 weeks old) were injected subcutaneously with $3X10^6$ cells (HCC827) suspended in 50% PBS, 50% matrigel and allowed to grow to 200-300mm^3 before treatment was started. Animals were randomly assigned to one of four groups: Vehicle, CB-839, Erlotinib, Erlotinib + CB-839. Animals were dosed for 6 day. Body weights (g) and caliper measurements ($(LxW^2)÷2 = mm^3$) were recorded twice a week. At the end of the study animal tissue was snap frozen in liquid nitrogen or fixed in 10% buffered formalin 2 hrs post final dose. Mice were housed in pathogen-free facilities at UCLA. All experimental procedures performed on mice were approved by the UCLA Animal Research Committee. The vehicle consisted of 25% (w/v) hydroxypropyl-β-cyclodextrin in 10 mmol/L citrate, pH 2. CB-839 was formulated as a solution at 20 mg/mL (w/v) in vehicle. Vehicle and CB-839 were provided by Calithera Biosciences. Erlotinib (Sellekem) was formulated in phosphate buffered saline. Mice were dosed with vehicle and CB-839 twice daily (9am and 5pm) and Erlotinib was dosed once daily (9am). CB-839 was delivered at 200mg/kg in all *in vivo* experiments and Erlotinib was delivered at 5 mg/kg/qd and 12.5 mg/kg/qd were noted. All drugs were administered by oral gavage.

PET Imaging

In vivo small animal imaging was conducted at the Crump Institute's Preclinical Imaging Technology Center. Mice underwent microPET (GENISYS 8 PET/CT, Sofie Biosciences) and microCT (CrumpCAT, Arion Hadjioannou laboratory) imaging with ^{11}C-L-glutamine and ^{18}F-fluorodeoxyglucose (^{18}F-FDG) on consecutive days both before and after six days of treatment. Briefly, mice were injected via lateral tail vein with radiolabeled probe (200-400 μCi for ^{11}C-L-glutamine and 70 μCi for ^{18}F-FDG), underwent 60 min uptake under 2% isoflurane anesthesia, followed by static microPET and microCT imaging. The microPET images were acquired for 600 sec with an energy window of 150-

650 keV, reconstructed using maximum-likelihood expectation maximization with corrections for photon attenuation, detector normalization and radioisotope decay (scatter correction was not applied) and converted to units of percent injected dose per gram (%ID/g). The microCT images were acquired under “high resolution” continuous mode using a 50 kVp, 200 μA X-ray source and reconstructed using the Feldkamp algorithm with a voxel size of 125 μm. Region-of-interest (ROI) analysis was conducted using AMIDE version 1.0.5 (Loening and Gambhir, 2003) on tumors and select normal tissues (liver, muscle, lung, heart, brain, and subcutaneous fat). To account for overall PET probe biodistribution variations between animals, tumor uptake was normalized to uptake in a reference tissue: muscle for ^{11}C-L-glutamine and liver for ^{18}F-FDG, as previously described (Venneti et al., 2015).

^{11}C-Glutamine synthesis

Synthesis of 5-[C-11]-GLN was based on a previously reported method (Qu et al., 2012) and performed on an in-house developed platform. Briefly, Carbon-11, was produced in an 11MeV RDS112 with a 14-N(p,a)11-C reaction in an aluminium target body. [C-11]CO_2 was converted to [C-11]-methane at 420 ^{o}C over a nickel catalyst. Using mass flow controllers, a mixture of [C-11]-methane and anhydrous ammonia gas was directed towards a platinum wire–packed quartz tube placed in a furnace at 980 ^{o}C at a total flow rate of 70cc/min with a 50/20 mixture of [C-11]-methane /Ammonia, generating [C-11]-HCN. [C-11]-HCN^{-} was trapped in the mixture of KOH/DMF (1mg/300 ul). 4mg of (S)-Tert-Butyl 2-((Tert-Butoxycarbonyl) Amino)-4-Iodobutanoate precursor, prepared in house, was added to the first reactor and heated to 115^{o} C for 5 minutes. The reaction mixture was cooled, diluted with 10 mL of H_2O and pushed through a C-18-classic Sep Pak. The cartridge was washed with H_2O (2x, 10 ml), dried with N_2 for 40 seconds and 1ml of MeCN was used to elute the intermediate [C-11]-nitrile, into a second reactor. Acetonitrile was evaporated at 115^{o} C under a gentle stream of N_2. The process of evaporation was repeated two times to ensure the complete azeotropic removal of H_2O and the mixture of 200 μl of TFA/H_2SO_4 (4/1) was added to the dry

residue. The mixture was heated at 115^{o} C for 10 minute, then cooled and diluted with 2ml of H_2O and pushed through ~3 g of Ag11-A8 resin (packed into 8x80 mm glass column and activated with 40 mL of 0.5 M NaCl and 200 ml of H_2O). 4ml of H_2O were used to elute the product which was collected in 1 ml fractions. The fraction, with a maximum of activity per 1 ml, contained 5-[C-11]-GLN with radiochemical purity >90% (*e.e.,* >95%) according to HPLC results (Phenomenex Chirex^{TM} 3147, 4.6x250 mm column; Mobile Phase: 2mM CusO4 in H_2O/EtOH (95/5); Flow Rate = 1 ml/min, Tr = 5.89) and had a pH = 7 with osmolality 300±50 milliosmoles/liter. The full synthesis and QC took approximately 55 minutes with RCY of 20-30% and SA of 2000 – 5000 Ci/mmol (decay corrected to EOB).

Mass Spectrometry

The experiments were performed as described (Thai et al., 2014). Briefly, 5-10mg of frozen tissue was homogenized in 1ml 80% methanol (-80°C). After 5 min centrifugation at top speed (4°C) supernatant was transferred to a separate tube. Tissue pellet was resuspended in SDS lysis buffer and protein content was measured using BCA kit (Thermo Scientific). Supernatant equivalent to 5ug of protein was transferred to a glass tube, 10nM of norvaline as added and samples were dried using EZ-2Elite evaporator. Dried samples were stored in -80°C freezer until further processing. For the mass spectrometry-based analysis of the sample, 5 ml were injected onto a Luna NH2 (150 mm x 2 mm, Phenomenex) column. The samples were analyzed with an UltiMate 3000RSLC (Thermo Scientific) coupled to a Q Exactive mass spectrometer (Thermo Scientific). The Q Exactive was run with polarity switching (+4.00 kV / -4.00 kV) in full scan mode with an m/z range of 70-1050. Separation was achieved using A) 5 mM NH_4AcO (pH 9.9) and B) ACN. The gradient started with 15% A) going to 90% A) over 18 min, followed by an isocratic step for 9 min. and reversal to the initial 15% A) for 7 min. Metabolites were quantified with TraceFinder 3.1 using accurate mass measurements (≤ 3 ppm) and retention times established by running pure standards. Data analysis,

including principal component analysis and hierarchical clustering was performed using the statistical language R.

Combination Index

Cells were treated with the indicated drug combinations and cell viability was measured after 72 hours using Cell Titre Glo. Combination Index values (CI) were calculated using Calcusyn Software (Biosoft) according to the methods of Chou and Talalay (Chou and Talalay, 1984). CI values < 1 indicate a synergistic drug-drug interaction.

Depletion of substrates in medium

For experiments quantifying metabolite consumption or production in tissue culture media, cells were incubated in complete medium with compounds in 0.5% DMSO for 24 hours. Drug concentrations were chosen based on the combination index and are as follows for H1650: vehicle, 62.4nM CB-839, and/or 1uM erlotinib and HCC827 as follows: 300nM CB-839, 12.5nM erlotinib. Media concentrations of glucose, lactate, glutamine, and glutamate were quantified using the YSI 2900 Biochemistry Analyzer (YSI Life Sciences) and cell counts were normalized to ViaCount (Millipore) assayed in parallel plates on a Guava cytometer (Millipore).

Seahorse oxygen consumption rates

To quantify rates of oxygen consumption, cells were seeded in complete medium with compounds on XF96 V3 PET plates (Seahorse Biosciences). After the cells incubated overnight, the medium was exchanged with fresh compounds in complete medium without FBS or bicarbonate. The plates were incubated without CO2 for 1 hour, then loaded on the Seahorse XF96 Bioanalyzer (Seahorse Biosciences) for quantification of oxygen consumption rates (OCR) and extracellular acidification rate (ECAR).

Immunoblotting

Lysates were prepared as previously described (Milica Momcilovic, 2015). Following antibodies were used: phospho-EGFR Y1068 (Cell Signaling, #3777), GLUT1 (Alpha Diagnostics # GT11-A), SLC1A5 (ASCT2) (Cell Signaling, #8057), SLC38A1 (Sigma, HPA052272**)** actin (Cell Signaling, #4970), phospho-AMPK T172 (Cell Signaling, #2535), AMPKa (Cell Signaling, #2532), phospho-Akt S473 (Cell Signaling, #4060), HKII (Cell Signaling, #2867), phospho-ULK1 S555 (Cell Signaling, #5869), LC3A/B (Cell Signaling, #4108), cleaved PARP (Cell Signaling, #5625), cleaved caspase-3 (Cell Signaling, #9661), p62 (Progen, GP62-C), Myc (Abcam, ab32072), HIF1a (Novus, NB100-449), GLS (Abcam, ab156876), Atg7 (Cell Signaling, #8558).

Immunohistochemistry

Tumors were excised and fixed for 16 hrs in 10% buffered formalin. Tissues were processed and embedded by Translational Pathology Core Laboratory (TPCL) at UCLA. Slides are stained following published protocol (Momcilovic et al Cancer Research 2015). Briefly, following deparafinization, antigen retrieval was performed by heat induced antigen retrieval method following manufacturers suggestions for each antibody. Endogenous peroxidase activity was quenched by incubating slides in 3% hydrogen peroxide for 10 min. Blocking was completed with 5% goat serum for 1hr at room temperature. Following incubation with primary and secondary antibodies, avidin-biotin peroxidase (ABC) complex (Vector Labs) was used. Finally, staining was visualized using the ImmPACT DAB (Vector Labs). Slides were counterstained with dilute hematoxylin. The following antibodies were used: Ki67 (1:200, SP6, Thermo), phospho-EGFR Y1068 (1:200, Cell Signaling, #3777), phospho-AMPK T172 (1:100, Cell Signaling, #2535), p62 (1:200, Progen, GP62-C). For phospho-AMPK staining SignalStain Boost Detection Reagent (Cell Signaling, #8114) and ImmPACT NovaRed (Vector Labs, #4805) were used. Following staining slides were digitally scanned onto a ScanScope AT (Aperio Technologies, Inc.). Digital slides were analyzed with the Definiens' Tissue Studio

(Definiens Inc.) to determine percent positive cells for Ki67 and phospho-EGFR Y1068 stains, and to quantify p62 staining.

Supplemental References:

Chou, T. C., and Talalay, P. (1984). Quantitative analysis of dose-effect relationships: the combined effects of multiple drugs or enzyme inhibitors. Adv Enzyme Regul *22*, 27-55.

Milica Momcilovic, R. M., Evan Abt, Atsuko Seki, Sarah A. Simko, Clara Magyar, David B. Stout, Michael C. Fishbein, Tonya C. Walser, Steven M. Dubinett and David B. Shackelford (2015). Heightening energetic stress selectively targets LKB1-deficient non-small cell lung cancers. Cancer Res *In Press*.

Qu, W., Oya, S., Lieberman, B. P., Ploessl, K., Wang, L., Wise, D. R., Divgi, C. R., Chodosh, L. A., Thompson, C. B., and Kung, H. F. (2012). Preparation and characterization of L-[5-11C]-glutamine for metabolic imaging of tumors. J Nucl Med *53*, 98-105.

Shackelford, D. B., Abt, E., Gerken, L., Vasquez, D. S., Seki, A., Leblanc, M., Wei, L., Fishbein, M. C., Czernin, J., Mischel, P. S., and Shaw, R. J. (2013). LKB1 inactivation dictates therapeutic response of non-small cell lung cancer to the metabolism drug phenformin. Cancer Cell *23*, 143-158.

Thai, M., Graham, N. A., Braas, D., Nehil, M., Komisopoulou, E., Kurdistani, S. K., McCormick, F., Graeber, T. G., and Christofk, H. R. (2014). Adenovirus E4ORF1-induced MYC activation promotes host cell anabolic glucose metabolism and virus replication. Cell Metab *19*, 694-701.